



## Supporting Information

for *Small*, DOI 10.1002/smll.202401998

Adsorbed Carbon Monoxide-Enabled Self-Terminated Au-Grafting on Pt<sub>6</sub> Nanoclusters for Enhanced Methanol Electrooxidation

*Paloli Mymoona, Edakkattuparambil Sidharth Shibu and Chinnaiah Jeyabharathi\**

## Supporting Information

Adsorbed Carbon Monoxide Enabled Self-Terminated Au-Grafting on Pt<sub>6</sub> Nanoclusters for Enhanced Methanol Electrooxidation

Paloli Mymoona, Edakkattuparambil Sidharth Shibu, Chinnaiah Jeyabharathi\*

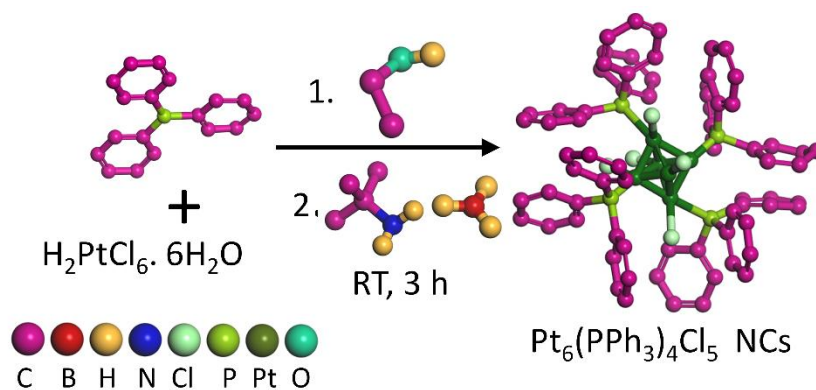


**Figure S1:** Scheme for the synthesis of  $\text{Pt}_6(\text{PPh}_3)_4\text{Cl}_5$ .

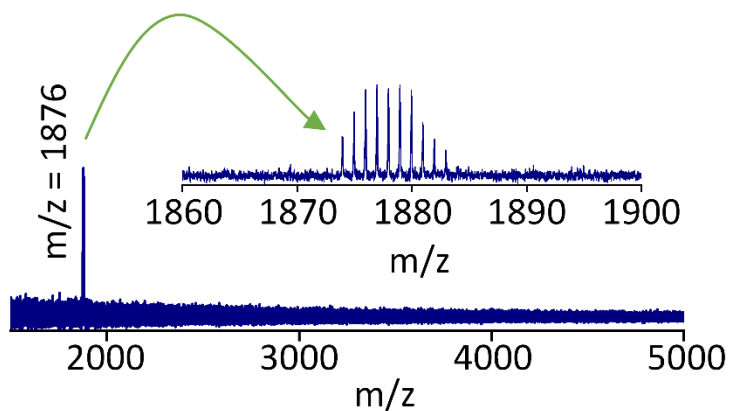


**Figure S2:** The MALDI-TOF mass spectrum of  $\text{Pt}_6(\text{PPh}_3)_4\text{Cl}_5$  and an enlarged view of the molecular ion peak is given in the inset.

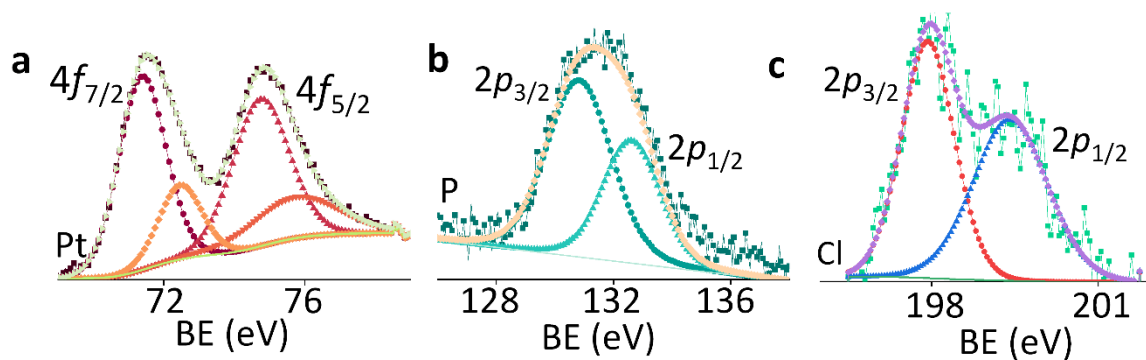


**Figure S3:** XPS of (a) Pt, (b) P, and (c) Au of Pt<sub>6</sub> NC/C.

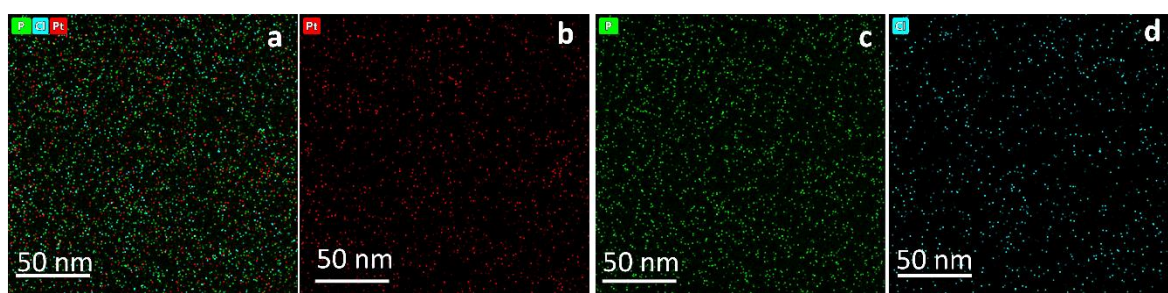


**Figure S4:** Element maps of Pt<sub>6</sub> NC showing distributions of Pt (red), P (green), and Cl (turquoise), respectively.

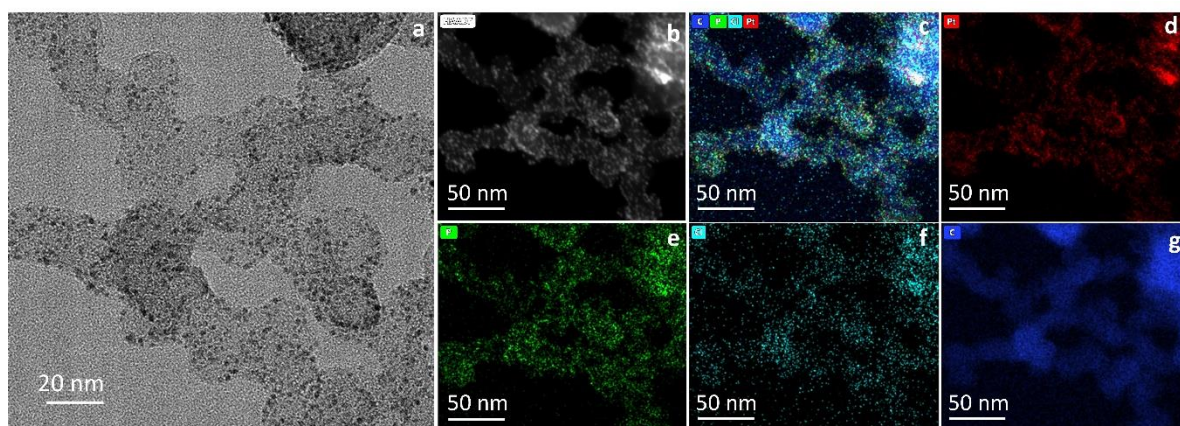


**Figure S5:** (a) HR-TEM (b) HAADF-STEM, and corresponding element maps of Pt<sub>6</sub> NC/C showing distributions of Pt (red), P (green), Cl (turquoise), and C (blue), respectively.

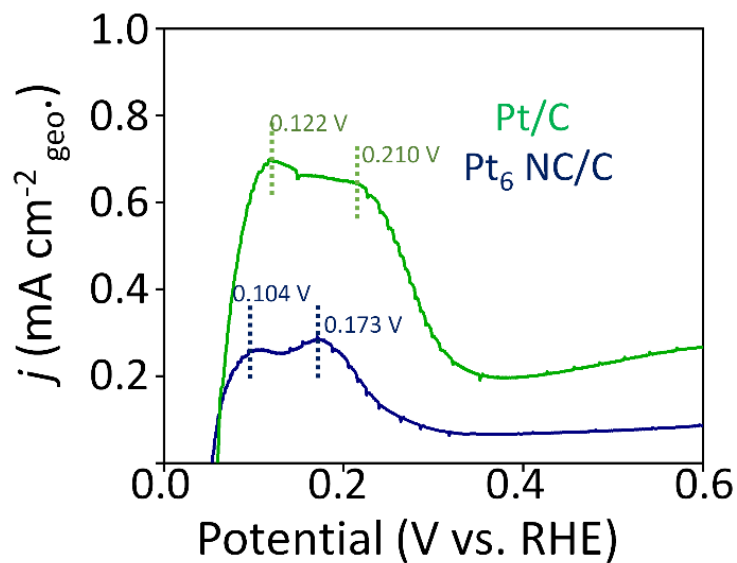


**Figure S6:** CV curves of Pt<sub>6</sub> NC/C and Pt/C in 0.1 M H<sub>2</sub>SO<sub>4</sub> at 100 mV s<sup>-1</sup> showing the hydrogen desorption region.

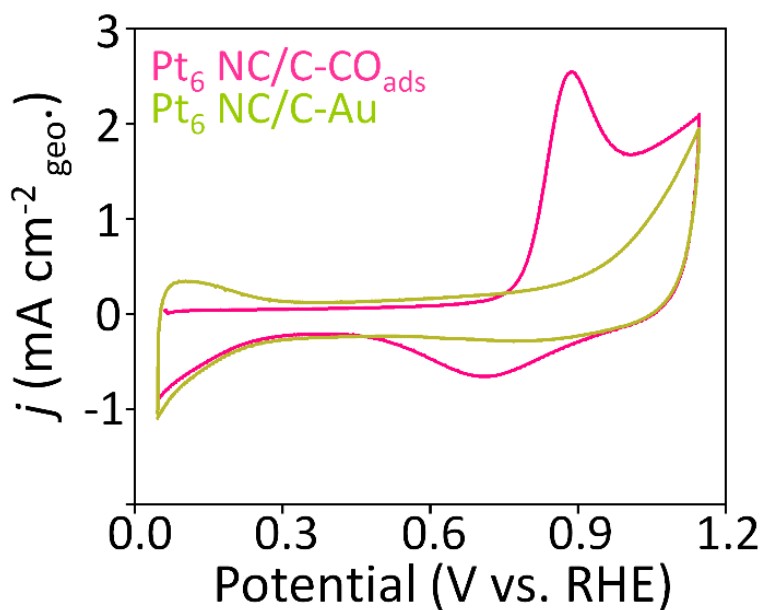


**Figure S7.** CO-stripping curves of Pt<sub>6</sub> NC/C in deaerated 0.1 M H<sub>2</sub>SO<sub>4</sub> at 50 mV s<sup>-1</sup> before and after Au decoration.

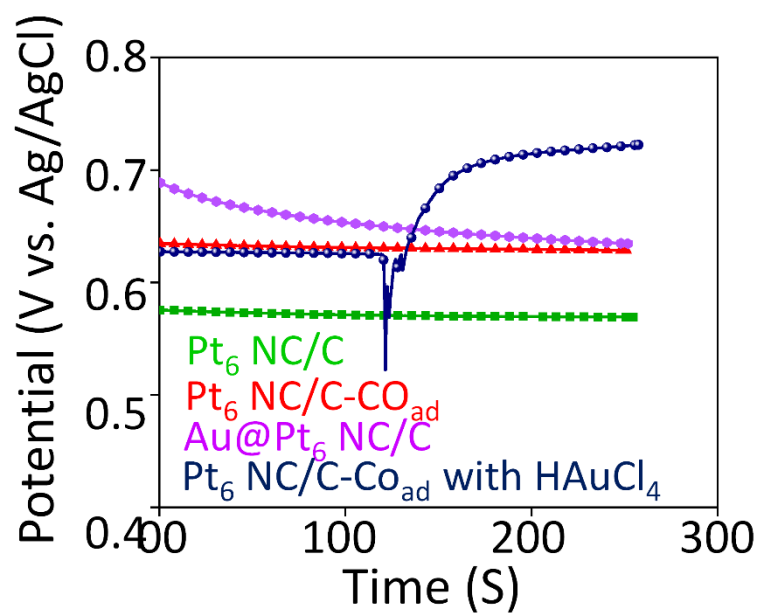


**Figure S8.** The OCV of Pt<sub>6</sub> NC/C, Pt<sub>6</sub> NC/C-CO<sub>ads</sub>, Au@Pt<sub>6</sub> NC/C, and Pt<sub>6</sub> NC/C-CO<sub>ads</sub>.

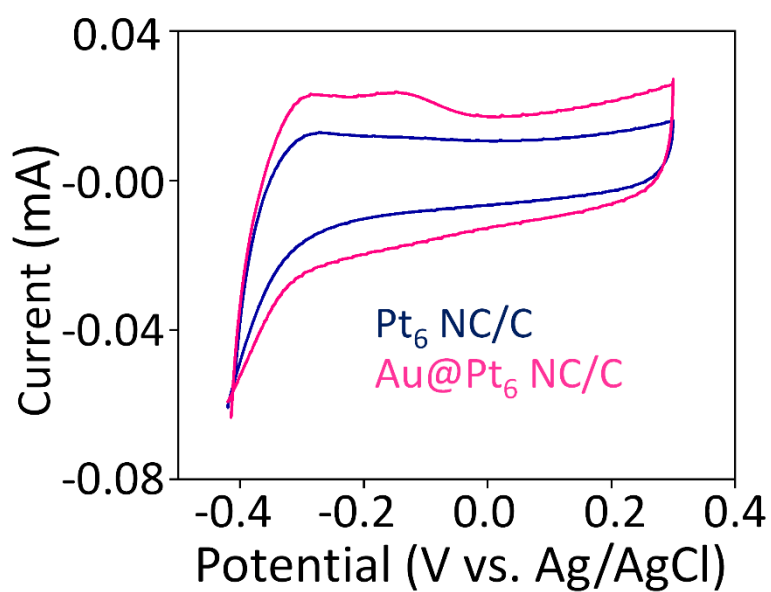


**Figure S9.** CV curves of Pb-UPD of Pt<sub>6</sub> NC/C and Au@Pt<sub>6</sub> NC/C at 20 mV s<sup>-1</sup>.

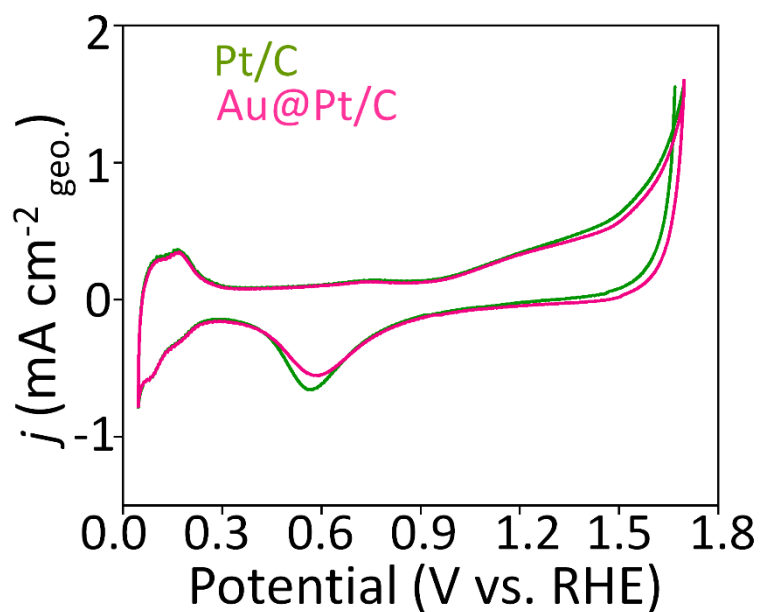


**Figure S10.** CV curves of Pt/C and Au@Pt/C in 0.1 M H<sub>2</sub>SO<sub>4</sub> at a scan rate of 100 mV s<sup>-1</sup> from 0.00 to 1.45 V<sub>RHE</sub>.

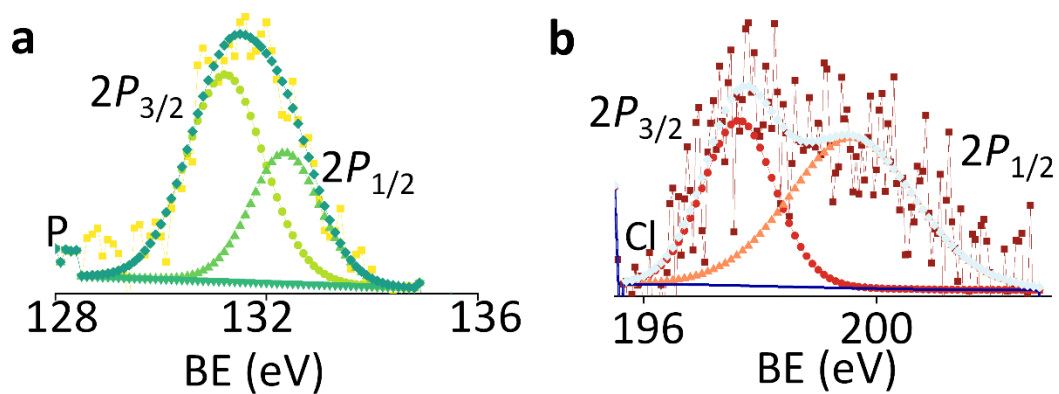


**Figure S11.** The XPS of (a) P 2*p* and (b) Cl 2*p* of Au@Pt<sub>6</sub> NC/C.

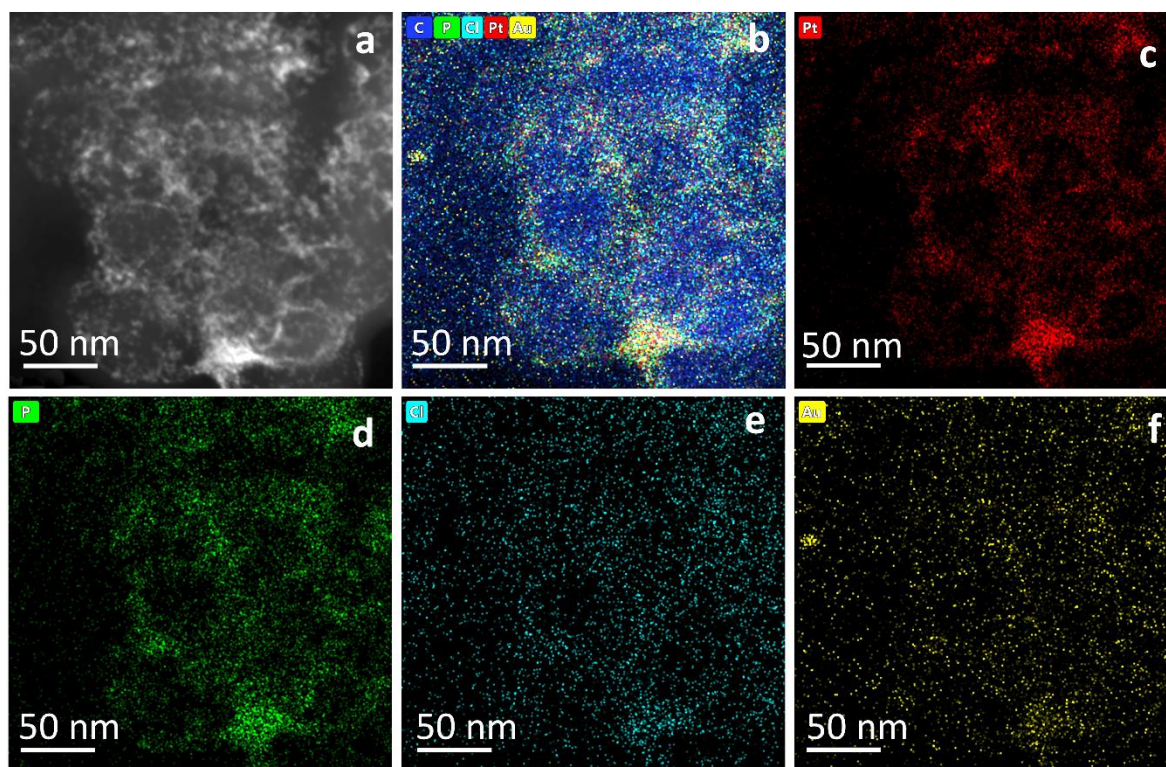


**Figure S12:** (a) HAADF-STEM and STEM-EDS mapping of the Au@Pt<sub>6</sub> NC/C shows the presence of (c) Pt, (d) P, (e) Cl, and (f) Au.

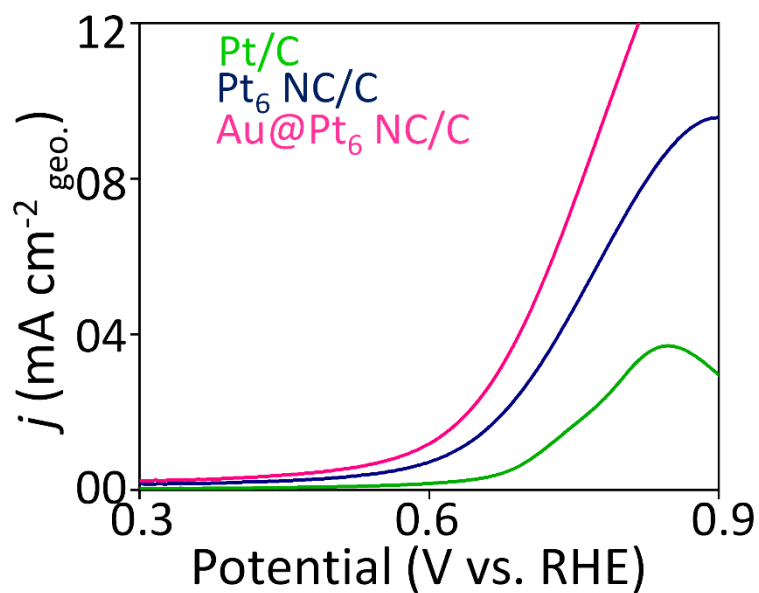


**Figure S13.** CV of Pt/C, Pt<sub>6</sub> NC/C, and Au@Pt<sub>6</sub> NC/C showing the MOR onset potential region.

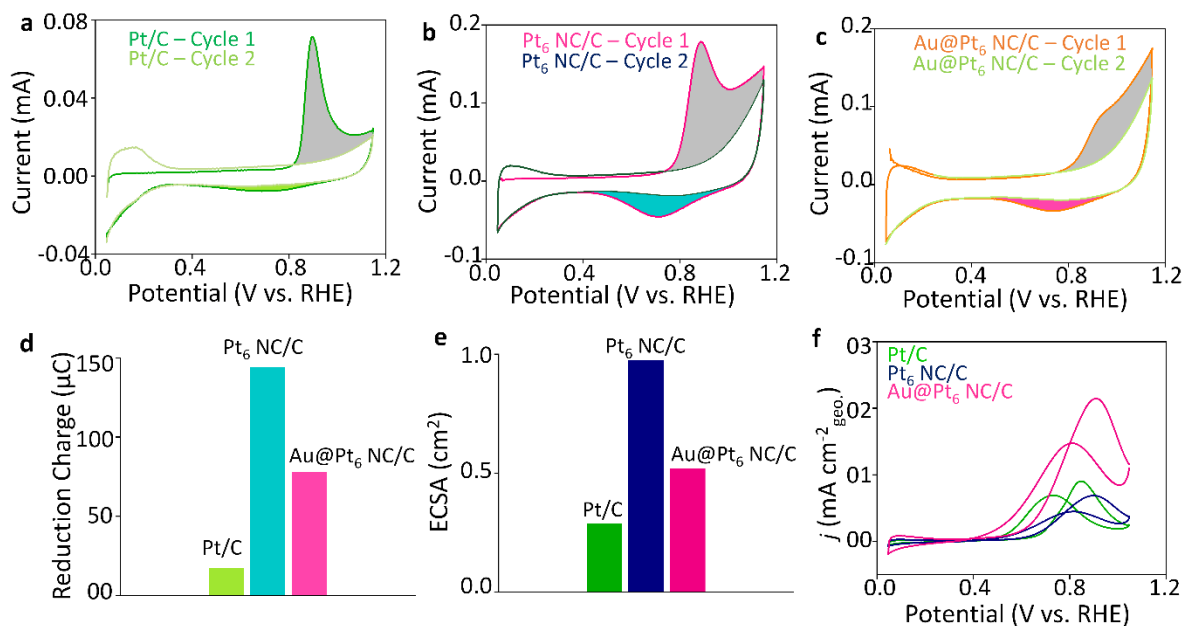


**Figure S14:** (a-c) CO-stripping curves of Pt/C, Pt<sub>6</sub> NC/C, and Pt<sub>6</sub> NC/C-Au in deaerated 0.1 M H<sub>2</sub>SO<sub>4</sub> at 50 mV s<sup>-1</sup>. Histogram representing (d) charge corresponding to oxide reduction and (e) ECSA of the Pt/C, Pt<sub>6</sub> NC/C, and Au@Pt<sub>6</sub> NC/C. (f) *i*R-corrected and ECSA normalized MOR curves of the Pt/C, Pt<sub>6</sub> NC/C, and Au@Pt<sub>6</sub> NC/C in 0.1 M H<sub>2</sub>SO<sub>4</sub> at 50 mV s<sup>-1</sup>.

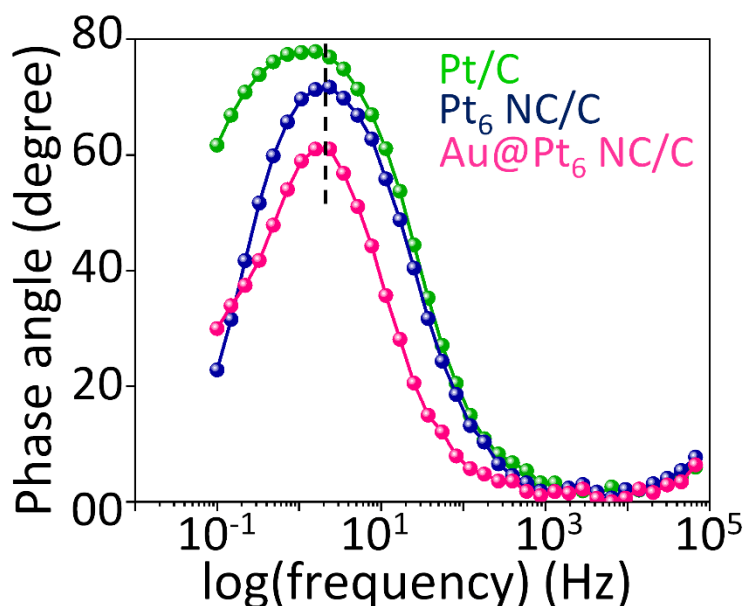


**Figure S15.** EIS Bode plot of Pt/C, Pt<sub>6</sub> NC/C, and Au@Pt<sub>6</sub> NC/C at 0.40 V<sub>Ag/AgCl</sub>

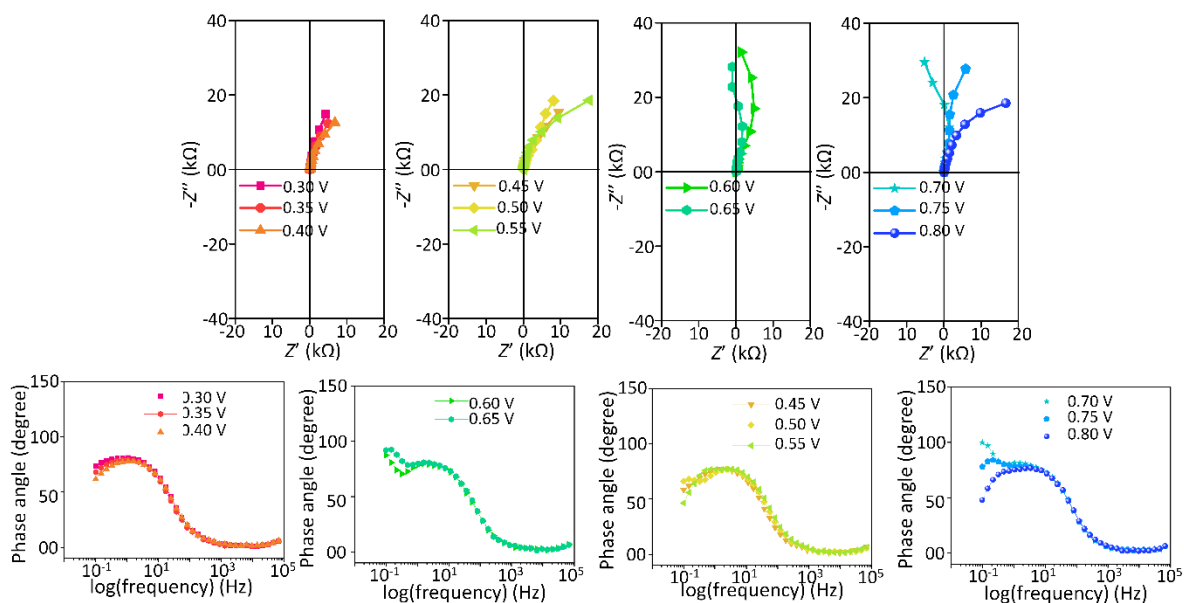


**Figure S16.** EIS Nyquist plot and Bode plot of Pt/C in 0.1 M H<sub>2</sub>SO<sub>4</sub> and 0.1 M methanol.

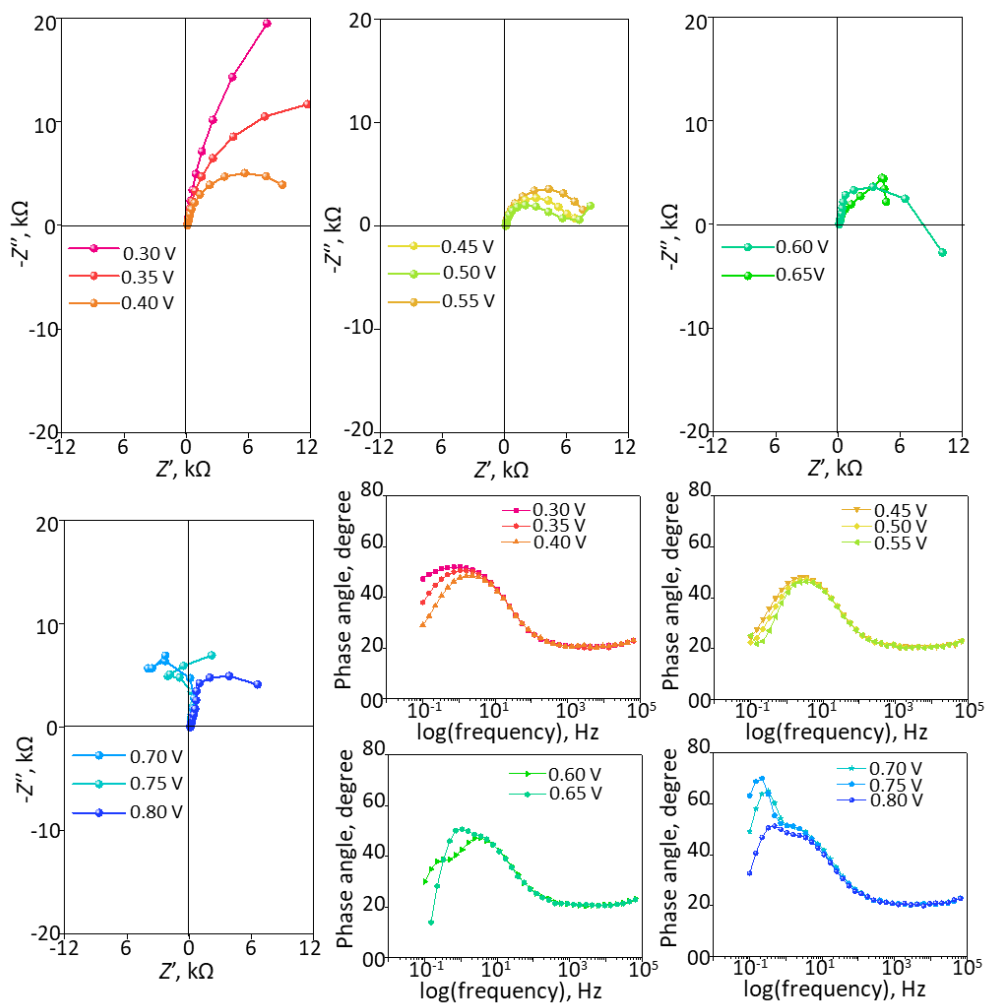


**Figure S17.** EIS Nyquist plot and Bode plot of Pt<sub>6</sub> NC/C in 0.1 M H<sub>2</sub>SO<sub>4</sub> and 0.1 M methanol.

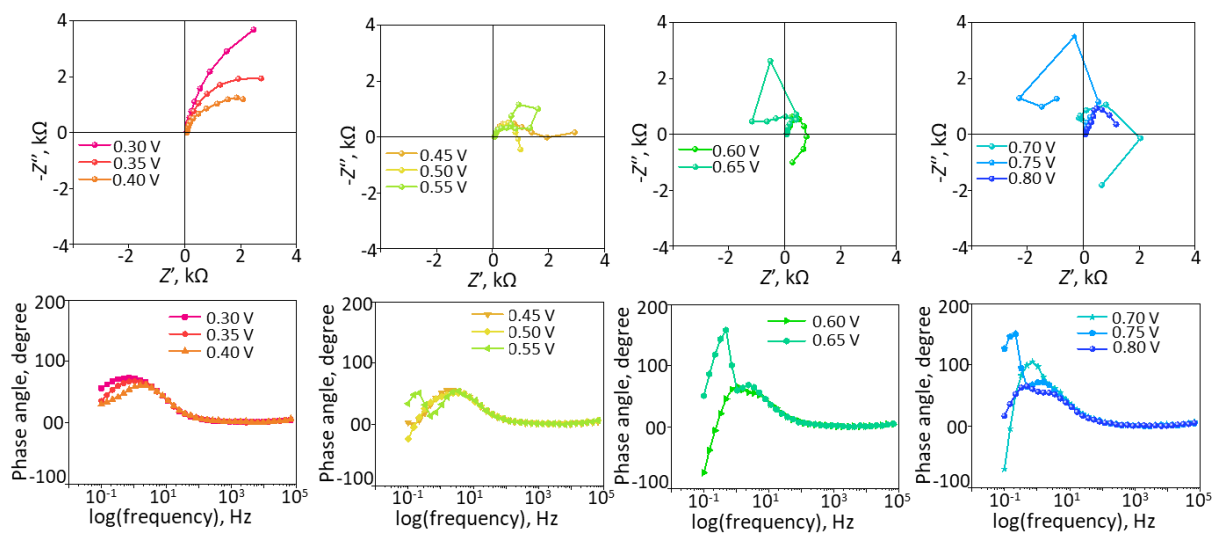


**Figure S18.** EIS Nyquist plot and Bode plot of Au@Pt<sub>6</sub> NC/C in 0.1 M H<sub>2</sub>SO<sub>4</sub> and 0.1 M methanol.

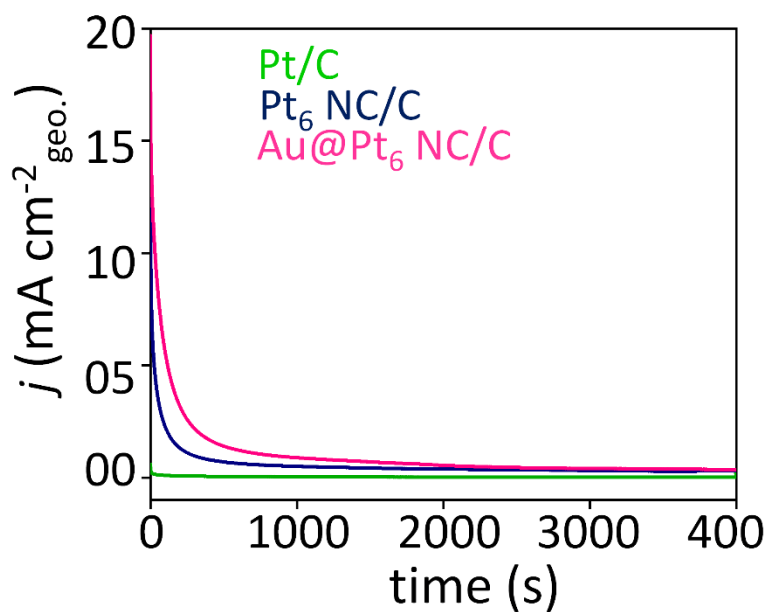


**Figure S19.** The CA MOR was conducted at 0.65 V<sub>Ag/AgCl</sub> under quiescent conditions for 4000 s.

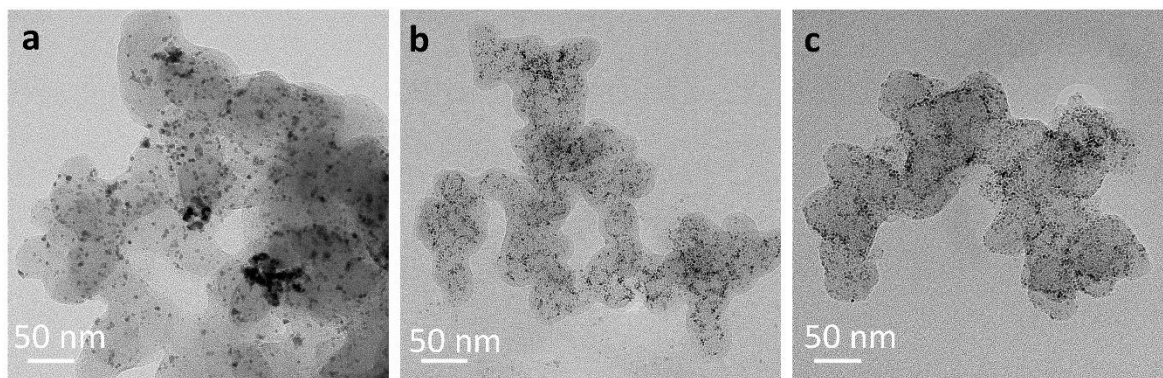


**Figure S20.** TEM of (a) Pt/C, (b) Pt<sub>6</sub> NC/C, and (c) Au@Pt<sub>6</sub> NC/C after CA test.

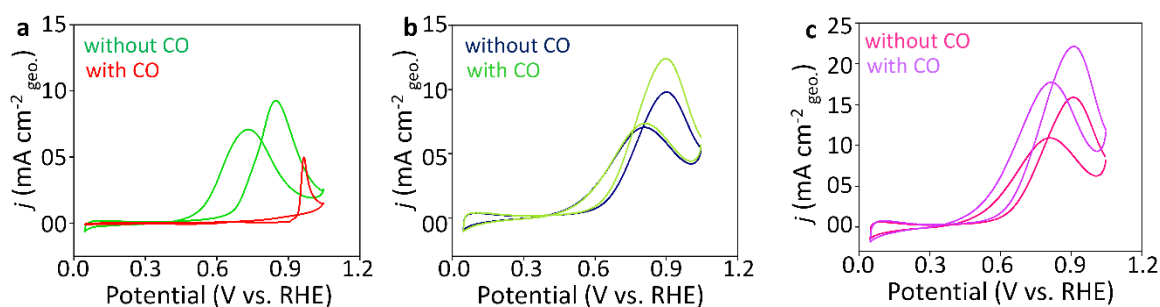


**Figure S21.** MOR curves of (a) Pt/C, (b) Pt<sub>6</sub> NC/C, and (c) Au@Pt<sub>6</sub> NC with CO and without CO.

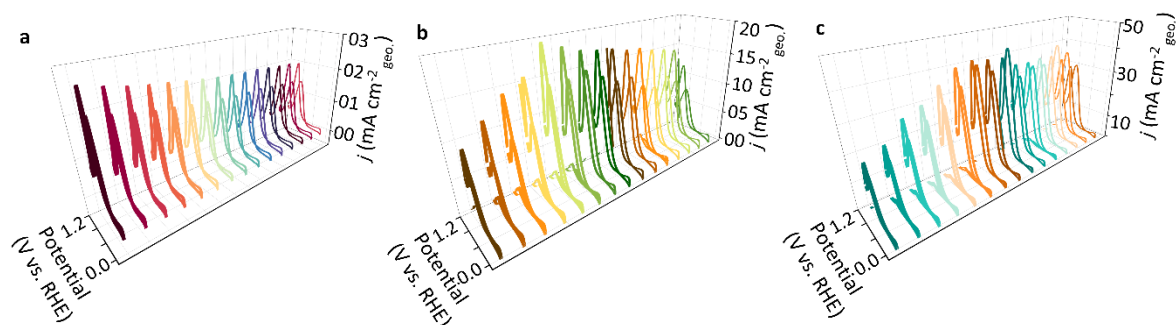


**Figure S22.** MOR curves of (a) Pt/C, (b) Pt<sub>6</sub> NC/C, and (c) Au@Pt<sub>6</sub> NC/C after each activation cycle.

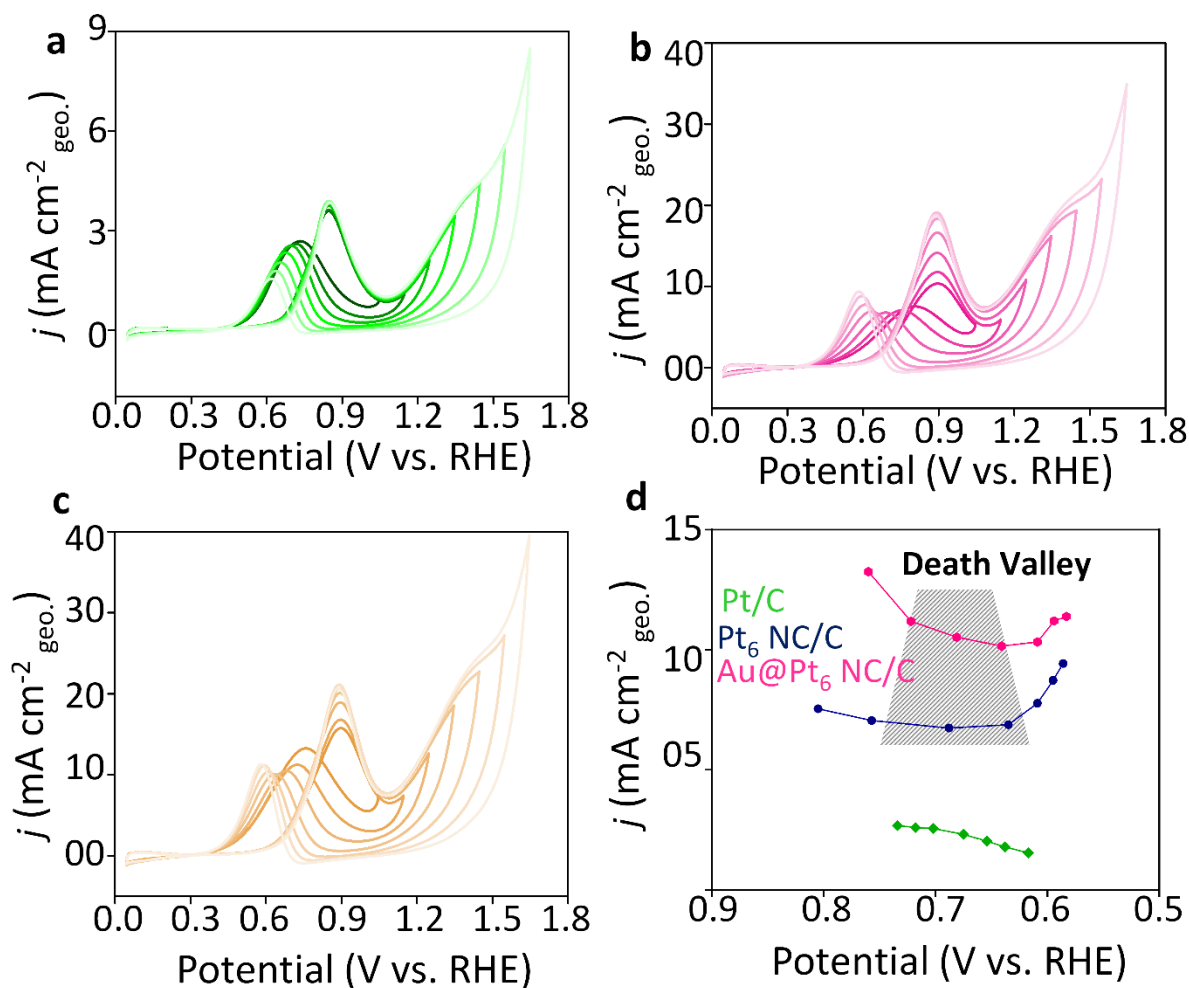


**Figure S23.** MOR curves of (a) Pt/C, (b) Pt<sub>6</sub> NC/C, and (c) Au@Pt<sub>6</sub> NC/C with different anodic limit potentials. (d) The plot of MOR peak current density values as a function of cathodic sweep peak potential.

Sample	Element	Orbital	Peak Area	RSF	Corrected Area	Total Corrected Area
Au@Pt <sub>6</sub> NCs	Pt	4f <sub>7/2</sub>	115056.83	8.65	13301.37	29315.05
		4f <sub>5/2</sub>	109053.14	6.81	16013.68	
	Au	4f <sub>7/2</sub>	22133.19	9.58	2310.35	5106.50
		4f <sub>5/2</sub>	21082.97	7.54	2796.15	
Total	Pt+Au	-	-	-	34421.55	Pt (85.16%) Au (14.84%)

**Table S1:** Calculation of atomic composition of Pt and Au of Au@P<sub>6</sub> NC/C from XPS data.

Catalyst	Oxidation Charge ( $Q_{ox}$ , $\mu\text{C}$ )	Oxide reduction Charge ( $Q_{red}$ , $\mu\text{C}$ )	CO-Stripping Charge ( $Q_{CO}$ , $\mu\text{C}$ )	Charge ( $Q_s$ , $\mu\text{C cm}^{-2}$ )	ECSA ( $\text{cm}^2$ )
Pt/C	137.6	17.94	119.66	420	0.2849
Pt <sub>6</sub> NC/C	553.8	144.2	409.6	420	0.9752
Au@Pt <sub>6</sub> NC/C	295.8	78	217.8	420	0.5185

**Table S2:** Calculation of ECSA of Pt/C, Pt<sub>6</sub> NC/C, and Au@Pt<sub>6</sub> NC/C.